

NEW APPROACHES TO THE STUDY OF CELLULOSE PYROLYSIS

R. J. Evans, F. A. Agblevor, H. L. Chum
Chemical Conversion Research Branch
Solar Energy Research Institute
Golden, Colorado 80401

J. B. Wooten, D. B. Chadwick and S. D. Baldwin
The Philip Morris Company
Richmond, Virginia 23261

KEY WORDS: Pyrolysis, Cellulose, Mass Spectrometry, Labeled Cellulose

INTRODUCTION

Cellulose pyrolysis presents some unique questions that include the effect of polymer secondary structure, (e.g., crystallinity), the intrinsic mechanism of pyrolysis by homolytic or heterolytic pathways, the role of alkali-metal catalysis, and the existence of major pathways, other than levoglucosan formation by "transglycosylation."¹⁻⁴ Most of the advances in the last five years have resulted from new analytical information. Piskorz et al.⁵ and Richards⁶ have published papers in recent years that describe hydroxyacetaldehyde formation as a major product and have speculated on the mechanism of this newly recognized, important product. These workers have used bench-scale pyrolysis units with physical collection of samples and employed chromatographic analysis of the products. Another approach is to perform pyrolysis with on-line analytical capability, either gas chromatography (Py-GC or Py-GC-MS) or mass spectrometry (Py-MS). Pouwels et al.⁷ have recently reported a detailed analysis of cellulose pyrolysis products using Py-GC-MS analysis. The major disadvantage of the GC approach is the collection of products on the head of the column where thermal degradation or other reactions can occur for some of the pyrolyzate constituents. The advantages of Py-MS are complete product collection and time-resolved analysis, but ambiguities arise due to the nature of the ionization method and the detection of products with the same nominal mass. The typical approach is to use low-voltage, electron ionization (12-25 eV) to preserve the parent ions as much as possible.⁸ When this approach is coupled with multivariate data analysis, it is often possible to deconvolute the major components among the products.⁹

We report here the implementation of several new tools for the study of cellulose pyrolysis using molecular beam mass spectrometry (MBMS).¹⁰ The new tools for py-MBMS investigations include systematic catalytic additions to identify correlated products, tandem mass spectrometry for identifying the contribution of specific compounds to nominal masses, preliminary rate analysis techniques for time-resolved data, and the growth and purification of ¹³C labeled cellulose using *Acetobacter xylinum* to be used in the study of cellulose pyrolysis.

EXPERIMENTAL

The MBMS and pyrolysis procedures have been previously described.¹⁰ A sample (1- 30 mg) contained in a quartz holder or "boat" is inserted into flowing (13 l/min at reactor temperature), preheated (typically 500°C) helium carrier gas. The hot gases are expanded through an orifice on the apex of a sampling cone into a low pressure chamber. The pressure difference is sufficient for free-jet expansion, which quenches the products and allows light gases, high-molecular-weight compounds, and reactive products to be simultaneously sampled and analyzed. A molecular beam, collimated through a second expansion, enters an ion source, where approximately 20 eV electron impact ionization is used to form ions. The mass range of interest (typically 15-300 amu) is scanned each second throughout the time for complete pyrolysis product evolution. Data are processed by integrating the spectra over the time of pyrolysis (10 to 90 s, depending on the sample and gas temperature), and by subtracting the background. If time-resolved data analysis is to be performed, each individual spectrum in a pyrolysis experiment is background-corrected. Factor analysis was used to analyze the results, either on a set of spectra from

related pyrolysis experiments to determine common behavior, or on time-resolved data to deconvolute different groups of products. The techniques used for factor analysis have been adapted from the methods of Windig and Meuzelaar⁸ that have been recently described by Windig.¹¹ The software package was the ISMA program¹¹ (Interactive Self-modeling Multivariate Analysis).

Avicel microcrystalline cellulose (FMC Corp., PH-102) was used throughout this work. Catalytic additions of salts were made by adding an appropriate amount of aqueous solution to just form a slurry and then allowing the material to dry completely in air at room temperature. Additions are reported as wt % cation relative to sample weight.

Cellulose was prepared with ¹³C at the C-1 position by growing cultures of *Acetobacter xylinum* on media that included D-[1-¹³C]-glucose. The cellulose sheets, or pellicles, were allowed to grow in media and then were thoroughly cleaned to remove other biopolymers and metal contamination. This cleaning procedure included autoclaving the pellicles in a solution of Alconox detergent followed by exhaustive washings in deionized water (resistivity = 10⁷ ohm). The pellicles were analyzed by C-13 NMR and found to be free of non-cellulosic carbon signals. The level of ¹³C₁ enrichment was 14%.

RESULTS AND DISCUSSION

The pyrolysis of cellulose is shown in figs. 1 and 2 for samples treated with different levels of KOH to demonstrate the two major product groups known to form: anhydrosugars and hydroxyacetaldehyde and their related compounds. The sample treated with 0.001% K has a product slate dominated by levoglucosan as shown by the average spectrum in fig 1B. Levoglucosan ionization fragment ions contribute to the intensity at m/z 144, 98, 73, 70, 60, and 57. The evolution profiles for m/z 43 and 144 are shown in fig. 1A as key markers for the two major product groups. In most natural cellulosic material, the yield of levoglucosan is less than that obtained from pure, isolated cellulose, such as Avicel. The average spectrum and time-resolved profiles for the pyrolysis products from cellulose treated with 0.5% K is shown in fig. 2. Hydroxyacetaldehyde, at m/z 60, fragments in the ion source to give fragment ions at m/z 31 and 32 and acetyl compounds give a major fragment ion at m/z 43. These masses are good indicators for the other major product slate. These data support the hypothesis that the level of alkali metals determine the relative amounts of these two major cellulose pyrolysis products. This point will be further demonstrated below.

A major question in cellulose pyrolysis is the existence of other "product classes" in cellulose pyrolysis. The systematic addition of catalytic alkali metal salt has been used to simulate the range of product groups encountered in cellulosic biomass pyrolysis. Salts investigated include NaCl, NaOH, KOH, and K₂CO₃ at the 0.001 to 0.1 wt. % level. Multivariate analysis of the average pyrolysis spectra was used to deconvolute three main groups of products. These catalysts show different mechanistic effects at various levels of addition. The factor score plot, the mass variable loading projections, and the variance diagram are shown in fig. 3. The score plot reveals a systematic effect from the catalytic addition with two trends and three main product groups. The three product groups are controlled by the level of salt addition. The mass-variable axes projections (fig. 3B) show that the masses are fanned out, which indicate that most masses belong to more than one of the three groups. The variance diagram (fig. 3C), which provides visual insight into the weighted average of the mass vectors, shows the three main maxima that indicate the direction of the component axes. The pure mass method is used to determine the vector coordinates that best represent the major, independent, real chemical "components." Chemical components in this application means suites of products that have correlated abundances in the spectra and hence appear to be controlled by the same chemical pathways. In this data set, three components were determined as represented by the pure masses, m/z 31, 144, and 191. The mathematically derived spectra of these three resolved components are shown in figs. 4-6, along with the relative amounts of these components for each sample.

The component spectrum 1 (fig. 4B) shows the key fragment ions at m/z 31, 32 and 43 that are due to the aldehyde and related structures. The plot of the relative concentration of component 1 for each sample as a function of wt % cation shows a systematic trend with higher yields at higher levels of alkali

metal. Six biomass samples (pine, fir, beech, maple, wheat straw, and bagasse) were analyzed along with the treated cellulose and were projected into the factor-analyzed cellulose results. These samples are included in fig. 4-6 as a function of their analyzed alkali metal concentrations. The resolved spectrum of component 2 in fig. 5B matches levoglucosan and shows higher relative concentrations in the samples with low levels of alkali metals that decreases monotonically with increased alkali-metal concentration. The biomass samples fit within this curve. Recent work^{5,6} has established that these two groups are the major products of cellulose pyrolysis, and our work shows that their relative amounts are controlled by alkali catalysis, which promotes the formation of the aldehydes at the expense of anhydrosugars. The results indicate a third product class that is also a function of alkali catalysis at low levels and that product group is shown in the component spectrum in fig. 6B. The peak at m/z 191 is of great interest since it is higher than the anhydrosugar weight of 162 and because it is an odd mass ion indicating either a protonated m/z 190 or a fragment ion of a higher mass, such as m/z 192. The peaks at m/z 173 and 163 and 145 are correlated with the intensity of m/z 191. The other major product is m/z 126, which could be 5-hydroxymethyl furfural, or hydroxybenzenes.¹² This will be discussed in relation to the CID of m/z 126. The peak at m/z 114 and fragment ion m/z 85 are common products from pentosan pyrolysis products and are thought to be due to a lactone.¹⁰ The relative concentration of component three shows a maximum at intermediate levels of cation concentration and the biomass samples show good agreement with the trends for the cellulose samples. These results imply that the pyrolytic behavior in biomass samples can be largely explained by these three product groups and that the effect of alkali-metal catalysis is sufficient to explain the control of the pyrolysis of cellulose in these materials.

Time-resolved data analysis can be used to estimate the relative kinetic rates for these different classes. As an initial application of this idea, the two sets of time-resolved spectra for the pyrolysis of cellulose treated with .001 and .5% K (as KOH) (shown in figs. 1A and 2A) were combined in the same data set and subjected to factor analysis to deconvolute the major trends as a function of reaction time. Only two significant chemical components were derived by this process in contrast to the three from the alkali-metal experiment. There are two possible reasons for this: 1) the third pathway was not active because these samples are from the two extremes of the sample distribution in fig. 3A, or 2) the two sets of time-resolved spectra did not contain sufficient variation to allow independent expression of the intermediate product group. The masses associated with the third product slate are divided between the other two. The mathematically derived spectra of the two components are shown in fig. 7 and clearly represent aldehyde and anhydrosugar product groups.

Using the relative yields of these two components in each spectrum the data are analyzed by plotting three calculated values that represent tests for zero, first, and fractional order rate behavior.¹³ The test for zero order is a plot of fractional conversion to products, expressed as

$$X_i = \left(\sum_{j=0}^i S_{1j} \right) / \left(\sum_{j=0}^n S_{nj} \right)$$

where S is the score for the j component ($j=1$ to 2, in this case) at time i, and n is the time for complete conversion. This can be subsequently converted to a first order test by plotting $-\ln(1-X_i)$ and as a fractional order test by plotting $(1-X_i)^{1/n}$, where n is the fractional order of reaction.¹³ The slope of the line can be converted to the rate constant when these values are plotted versus time, and straight line behavior is observed. In these experiments, there is a nonisothermal period while the sample is heated to the reactor temperature. The initial portion of the time-resolved behavior is therefore ignored. This method should be considered a screening technique since there are several uncontrolled factors (e.g., temperature of reacting solid, mass transfer, etc.) that prevent the calculation of intrinsic chemical kinetics with certainty. However, this rapid analytical approach is a way of comparing samples that sheds light on the chemical processes and utilize data that in the past were ignored. The use of factor analysis to deconvolute chemically specific information from time-resolved data is an improvement over weight loss rate analysis. Plots of these calculated values versus time are shown in fig. 8 for the evolution of the aldehydes component from the 0.5% K-treated cellulose and the anhydrosugar component for the 0.001% K-treated cellulose. In both the 0.001% K and 0.5% K samples, a reaction order of .8 and a rate constants of $0.17(\pm 0.02) \text{ s}^{-1}$ were calculated for the anhydrosugars. For the aldehydes, a reaction order of 0.4 and rates of 0.07 to 0.11 s^{-1} were obtained for the 0.001% and 0.5% samples, respectively. The

difference in rates for the aldehydes, if statistically significant, is not unreasonable if one assumes a more "zero-order nature" for the formation of hydroxyacetaldehyde, which is dependent on catalytic activity. The reproducibility of the reaction order for the two reactions under extremes of reaction is illustrative of the insight that this rate analysis of time-resolved data can provide.

Collision induced dissociation (CID) of selected ions has been used to deconvolute ambiguous peaks in pyrolysis-mass spectrometry of cellulose, such as m/z 60, 126, 144, and 162, which are known to be due to more than one product, and m/z 191, 163, and 145, which appear to have new significance in light of results reported above. The results are presented in table 1 for a variety of materials. The species at m/z 191 gives rise to fragments at m/z 173 and 163, due to a loss of 18 and 28, respectively. The series of daughter ions of m/z 191, at m/z 163, 145, and 127, resemble the dehydration series from the electron ionization fragment ions of levoglucosan at m/z 162, 144, and 126. This may imply that the parent of m/z 191 (m/z 192?) may be a derivative from an anhydrosugar. The peak at m/z 163 may be an electron ionization fragment of the same species that gives rise to m/z 191 and it also has daughter ions at m/z 145 and 127, but with a new daughter at m/z 85. Comparing m/z 162 from levoglucosan and cellulose indicates some dramatic differences with the cellulose ion giving rise to a daughter at m/z 73 that is not produced from levoglucosan. The parent at m/z 145 from cellulose pyrolysis is also different from the m/z 145 ion from levoglucosan, which again may be due to the m/z 145 being derived from the same species that gives rise to m/z 191. The daughters of m/z 144 are also more complicated from cellulose than levoglucosan. The model compounds at m/z 126 show relatively unique daughters for each (1,2,3-trihydroxybenzene - m/z 108; 1,3,5-trihydroxybenzene - m/z 85; 5-HMF - m/z 97; levoglucosenone - m/z 98). Untreated Avicel yields m/z 97 as a daughter of m/z 126, which indicates the 5-HMF and no hydroxybenzenes. The presence of salts lowers the overall daughter ion abundance from m/z 126, and the presence of m/z 108 would indicate the trihydroxybenzene in addition to 5-HMF. It is not generally recognized that the furfurals can arise from alkali metal catalysis, but these data support that hypothesis. The daughters of m/z 60 are also fairly unique for the model compounds and show that the daughters from treated cellulose can be resolved into the relative amounts of levoglucosan, hydroxyacetaldehyde, and acetic acid by the relative amounts of m/z 42, 32, and 45. Factor-analysis-based methods are being developed for deconvoluting CID spectra due to multiple products present at the nominal mass of interest.

Recent pyrolysis MBMS experiments of Acetobacter cellulose, grown on D-[1-¹³C]-glucose media are reported here and this is a most exciting new tool for PY-MS studies of cellulose pyrolysis. The selectively enriched, labeled and unlabeled Acetobacter cellulose samples were prepared and purified by the same methods to remove potential metal ion contaminants and to insure that both samples could be compared. The regular and ¹³C₁ Acetobacter cellulose samples were pyrolyzed in triplicate at 520°C in flowing helium. The sample size was approximately 5 mg. Since m/z 145 and 127 are associated with another product group (that is alkali-catalyzed) in addition to being the isotope peaks of m/z 144 and 126, respectively, the enrichment effect can be masked by the differences between samples in the level of inorganic contamination. The ratio of m/z 126/144 is a sensitive indicator of the relative amounts of these different product groups. The data in table 2 show that the ratios of m/z 126/144 are 0.53 and 0.50 for the regular and enriched Acetobacter cellulose samples, respectively. This leads to the conclusion that there is no significant difference between the two samples in the relative amounts of the major pyrolysis product groups. Therefore, the differences in table 2 that are statistically significant are due to the isotope enrichment at the C₁ position. The average spectrum for the replicates of regular cellulose pyrolysis is indicative of anhydrosugar formation (there was a low abundance of m/z 43, which is a confirmation that these are clean samples). Therefore, isotope effects from this sample will only be relevant to part of the range of cellulose pyrolysis products. An analysis of variance (ANOVA) was performed for the triplicate runs for the two samples. The results are presented as the F-ratio, which is a statistical parameter used to estimate the probability of significant differences between two or more classes of replicated samples. For this experiment, an F-ratio of 7.71 indicates 95% confidence that the measured difference is significant and an F-ratio of 21.2 implies 99% confidence. The ions with an F-ratio greater than 3.5 are included in tables 2 and 3. The F-ratio test shows significant enrichment at m/z 144 with an F-ratio of 87 for m/z 145 and 69 for m/z 144. Since this ion is a six carbon product, which must contain C₁, this verifies that the enrichment can be detected for C₁ containing species. Simulation

data are included in the tables that assume 14% enrichment and the presence of C₁ in the products at every mass. Note that the peak intensities are very close for m/z 144 and 145 for the labeled Acetobacter average and those in the simulated enrichment. The products at m/z 126 also contain six carbon atoms and again the enrichment values for m/z 126 and 127 closely match the simulated values. Of the lower molecular weight products, only m/z 98 is significantly higher.

To force the distribution of pyrolysis products to the aldehyde product slate, samples of the Acetobacter cellulose were treated with 0.1% KOH and treated similarly to the samples described above. In this sample, m/z 126 shows significant enrichment, but no low-molecular-weight products are higher in the enriched cellulose. This indicates that the m/z 60 products that are present under these alkali-catalyzed conditions are not formed from the C₁ position in cellulose, and glycolaldehyde must come from the C₂ to C₆ positions. This work is continuing with labeled cellulose at other carbon positions.

In summary, the use of systematic catalytic additions to promote formation of product groups, the use of rate analysis of time-resolved data, and the use of CID for characterization, improves the application of Py-MS as a tool for studying the chemistry of cellulose pyrolysis. The most exciting new development is the use of ¹³C-labeled cellulose that has specifically labeled positions and allows the source of each pyrolysis product to be traced to the exact position in the cellulose structure.

ACKNOWLEDGMENTS

The assistance of Carolyn Elam, David Gratson, Dingneng Wang, and Kuni Tatsumoto in experimental work, and of Willem Windig in discussions of multivariate analysis and use of the ISMA program is greatly appreciated.

REFERENCES

1. Antal, M. J., Jr. In Advances in Solar Energy; Boer, K. W.; Duffier, J. A., Eds.; Plenum: New York, 1985, vol.2, pp 175-728.
2. Shafizadeh, F. Applied Polymer Symposium 1975, 28, 153-174.
3. Kilzer, F. J.; Broido, A. Pyrodynamics 1965, 2, 151-163.
4. Golova, O. P. Russian Chemical Reviews, 1975, 44(8), 687-697.
5. Piskorz, J.; Radlein, D.; Scott, D. S. J. Anal. Appl. Pyrol. 1986, 9, 121-137.
6. Richards, G. N. Ibidem. 1987, 10, 251-255.
7. Pouwels, A. D.; Eikje, G. B.; Boon, J. J. Ibidem. 1989, 14, 237-280.
8. Meuzelaar, H. L. C.; Kistemaker, P. G. Anal. Chem. 1973, 45, 587-590.
9. Windig, W.; Meuzelaar, H. L. C. Ibidem. 1984, 56, 2297-2303.
10. Evans, R. J.; Milne, T. A. Energy Fuels 1987, 1, 123-137.
11. Windig, W.; Lippert, J. L.; Robbins M. J.; Kresinske, K. R.; Twist, J. P.; Snyder, A. P. Chemometrics and Intelligent Laboratory Systems, 1990, 9, 7-30.
12. Richards, G. N.; Shafizadeh, F.; Stevenson, T. T. Carbohydr. Res. 1983, 117, 322-327.
13. Carlson, L.; Feldthus, A.; Bo, P. J. Anal. Appl. Pyrol. 1989, 15, 373-381.

Table 1. Results of CID-MS on key masses from the pyrolysis of cellulose and selected model compounds. Conditions for CID were Argon collision gas and ion energies of approximately 20 eV. The intensities are relative to a parent ion intensity of 1000.

Parent	Material	Daughter Ions: m/z(intensity)
191	Avicel	127(168) 173(134) 145(113) 163(31)*
163	Avicel	145(112) 85(62) 127(36) 91(24)*
162	Avicel	73(44) 98(42) 144(42) 89(26)*
162	Levoglucozan	98(273) 116(114) 70(57) 106(52)
145	Avicel	85(77) 127(47) 99(34) 73(31)*
145	Levoglucozan	73(223) 98(89) 74(79)*
144	Avicel	72(92) 98(70) 73(57)*
144	Levoglucozan	73(144) 98(123)*
126	1,2,3-THB ¹	108(26) 80(26) 125(7)
126	1,3,5-THB ¹	85(20) 98(7) 125(7)
126	5-H-M-Furfural	97(486) 69(45) 125(11)
126	Levoglucozenone	98(281) 95(53) 80(48) 70(42) 97(41)
126	Avicel	97(121) 98(46) 80(41) 69(18) 81(11) 70(11)
126	cel+.05%Na ₂ CO ₃	97(34) 80(21) 98(12) 108(12)*
126	cel+.5%K ₂ CO ₃	98(20) 80(16) 97(14) 125(9)* 108(7)*
126	cel+.05%NaCl	97(59) 98(22) 80(13) 125(10) 108(7)*
126	Aceto. Cel#1	97(179) 98(45) 80(35) 69(33)
126	Aceto. Cel#2	97(109) 98(61) 69(25) 80(24) 70(16) 111(15)
60	Acetic Acid	45(533) 43(259) 42(48) 16(36) 15(12)
60	Hydroxyacetal.	32(1200) 31(873) 45(88) 43(35) 29(34) 42(32)
60	MeFormate	31(650) 32(477) 30(298) 29(75) 45(8) 15(6)
60	2-propanol	45(1700) 44(381) 31(202) 32(142) 43(80)
60	Levoglucozan	42(124) 31(60) 30(11)
60	Cel+.05%Na ₂ CO ₃	42(108) 31(73) 32(32) 45(16) 43(9) 30(8)*

*These peaks have low signal-to-noise and their identification as daughters should be considered tentative.

¹trihydroxybenzene

Table 2. Significant differences in the relative yields of pyrolysis products in regular ($I_{(m/z)R}$) and $^{13}C_1$ -enriched ($I_{(m/z)E}$) Acetobacter xylinum cellulose. Each sample was run in triplicate and analysis of variance was performed to determine the degree of statistical significance (F-ratio, Level of Significance: 21.2, 1%; 12.2, 2.5%; 7.71, 5%). The difference between these values shows the effect of enrichment. Simulated values ($I_{(m/z)S}$) are presented as if each mass was enriched by 14% in $^{13}C_1$.

m/z	Experimental				Simulated	
	$I_{(m/z)R}$	$I_{(m/z)E}$	F-ratio	$(I_{(m/z)R} - I_{(m/z)E})$	$I_{(m/z)S}$	$(I_{(m/z)R} - I_{(m/z)S})$
43	1.37	1.19	37.8	0.18	1.33	0.04
55	1.37	1.25	6.3	0.12	1.23	0.14
68	1.16	1.08	5.1	0.08	1.00	0.16
90	0.39	0.51	7.5	-0.11	0.48	-0.09
99	1.35	1.52	19.0	-0.16	2.38	-1.03
101	0.86	0.72	6.2	0.13	0.78	0.08
103	0.50	0.61	4.9	-0.11	0.57	-0.08
113	1.36	1.18	23.8	0.18	1.22	0.14
114	2.02	1.87	6.4	0.16	1.93	0.09
116	1.37	1.52	9.8	-0.15	1.41	-0.04
126	2.90	2.38	4.8	0.52	2.53	0.38
127	0.56	0.91	37.7	-0.35	0.89	-0.33
142	0.31	0.22	3.6	0.10	0.27	0.04
144	5.50	4.72	68.5	0.78	4.76	0.75
145	0.84	1.46	87.8	-0.62	1.49	-0.65
146	0.20	0.29	39.2	-0.09	0.29	-0.09
163	0.30	0.37	3.6	-0.07	0.30	0.00
167	0.22	0.15	4.1	0.07	0.20	0.02
192	0.16	0.23	22.0	-0.07	0.17	-0.01

Table 3. Significant differences in the relative yields of pyrolysis products in regular and $^{13}C_1$ -enriched Acetobacter xylinum cellulose treated with 0.1% KOH. See Table 2 caption for details.

m/z	Experimental				Simulated	
	$I_{(m/z)R}$	$I_{(m/z)E}$	F-ratio	$(I_{(m/z)R} - I_{(m/z)E})$	$I_{(m/z)S}$	$(I_{(m/z)R} - I_{(m/z)S})$
29	1.49	1.65	5.3	-0.16	1.50	-0.01
45	0.96	1.26	5.4	-0.30	1.44	-0.48
57	3.14	2.83	21.1	0.31	2.87	0.27
68	1.00	0.86	19.7	0.14	0.91	0.09
74	1.43	1.30	18.2	0.13	1.60	-0.17
85	2.52	2.36	19.0	0.16	2.43	0.09
97	1.80	1.60	6.0	0.19	1.71	0.08
98	3.58	3.32	18.1	0.25	3.33	0.25
126	3.35	2.60	11.8	0.74	2.93	0.41
127	0.59	0.95	34.4	-0.36	0.97	-0.39
142	0.26	0.21	41.7	0.04	0.24	0.02
144	0.80	0.48	20.5	0.32	0.71	0.09
145	0.43	0.33	5.3	0.10	0.48	-0.05
190	0.15	0.20	7.9	-0.06	0.14	0.01
191	0.14	0.17	120.	-0.04	0.14	-0.00

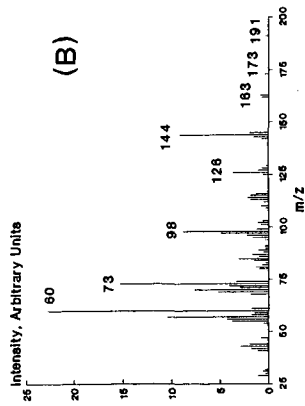
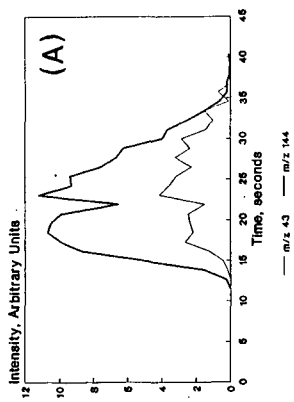


Fig. 1. The pyrolysis of Avicel cellulose treated with .001% K (as KOH) at 540 °C: (A) time-resolved evolution profile of m/z 43 and 144. (B) the average, background-corrected spectrum of pyrolysis products.

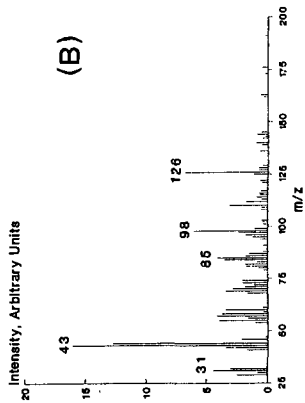
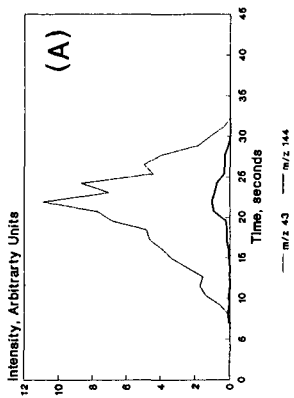


Fig. 2. The pyrolysis of Avicel cellulose treated with .5% K (as KOH) at 540 °C: (A) time-resolved evolution profile of m/z 43 and 144. (B) the average, background-corrected spectrum of pyrolysis products.

Effect of Salts on Cellulose Pyrolysis

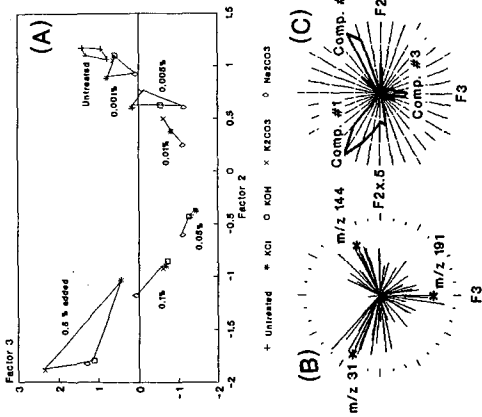


Fig. 3. The results of factor analysis of pyrolysis-mass spectra of avicel cellulose treated with different salts. The trajectories in (A) plot are shown in the data set; (B) mass variable loading projections showing underlying distribution of data set; and (C) the variance diagram, which is a weighted display of the mass axes projections and shows the maxima of clustering, which indicate the direction of component separation. The dashed lines which delineate component axis, are noted with asterisk in B.

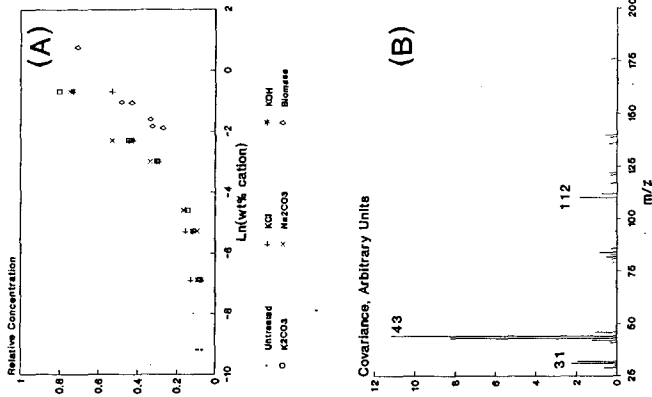


Fig. 4. The first component mathematically resolved from the data set in Fig. 3 (pure mass m/z 31) showing its relative concentration in the samples (A) and the reconstructed spectrum (B).

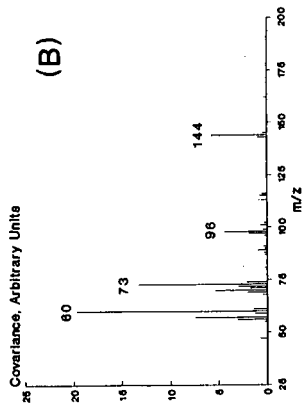
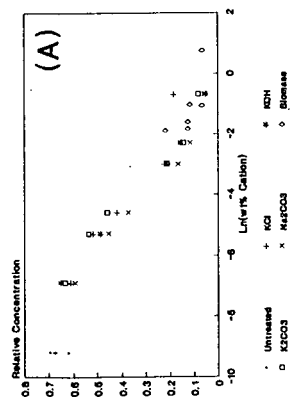


Fig. 5. The second component mathematically resolved from the data set in Fig. 3 (pure mass m/z 144) showing its relative concentration in the samples (A) and the reconstructed spectrum (B).

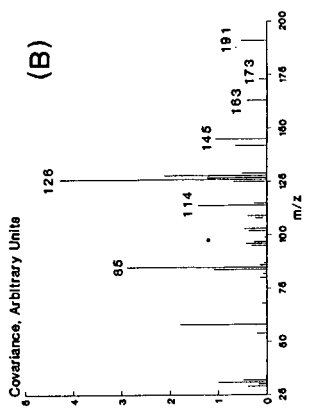
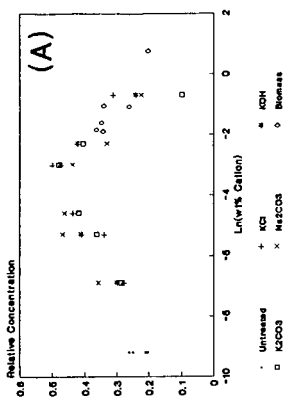
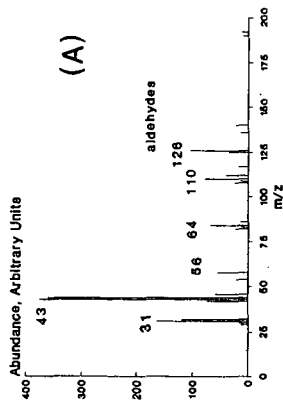


Fig. 6. The third component mathematically resolved from the data set in Fig. 3 (pure mass m/z 191) showing its relative concentration in the samples (A) and the reconstructed spectrum (B).

Component Spectrum 1



Component Spectrum 2

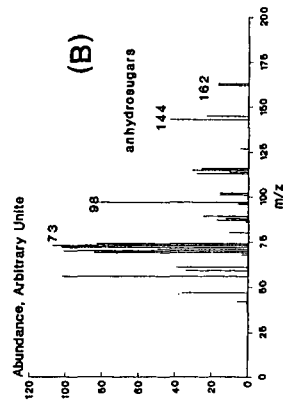


Fig. 7. The results of factor analysis on time resolved data for the .001% and .5% K-treated cellulose data sets, which were combined in one data set to deconvolute the major product species: (A) component spectrum 1, which represents the aldehydes; (B) component spectrum 2, which represents the anhydro sugars.

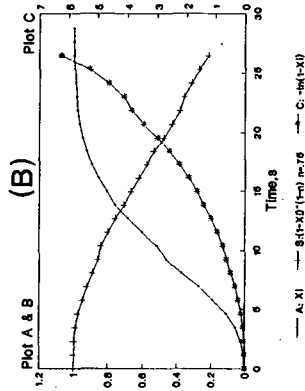
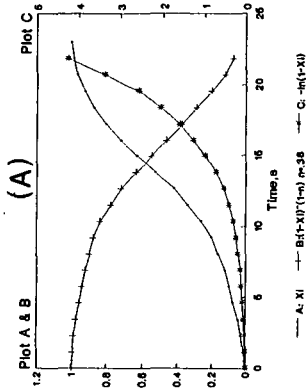


Fig. 8. Examples of the analysis of the rate of formation of the resolved components that are shown in fig. 7: (A) aldehydes from .5% K-treated cellulose and (B) anhydro sugars from .001% K-treated cellulose.